Pseudo-Jahn–Teller instability in the axial Fe^+ center in $KTaO_3$

A. Trueba,[1] P. García-Fernández,[1] M. T. Barriuso,[2] M. Moreno,[1] and J. A. Aramburu[1]
[1]*Departamento de Ciencias de la Tierra y Física de la Materia Condensada, Universidad de Cantabria, Avda. de los Castros s/n, 39005 Santander, Spain*
[2]*Departamento de Física Moderna, Universidad de Cantabria, Avda. de los Castros s/n, 39005 Santander, Spain*
(Received 18 May 2009; revised manuscript received 2 July 2009; published 31 July 2009)

The nature of the axial Fe4/2 center in $KTaO_3$, detected by electron-paramagnetic resonance experiments, has been a source of conflict until recently. Density-functional-theory calculations strongly support the model that ascribes such center to a Fe^+ impurity ($3d^7$ configuration) which enters the K^+ site and spontaneously moves off-center along a ⟨100⟩-type direction. This work is aimed at clarifying what are the main mechanisms responsible for such off-center instability using pseudo-Jahn–Teller theory. We find that the mixing of $3d_{x2-y2}$ and $3d_{xy}$ orbitals of iron ion with odd oxygen orbitals favored by the off-center displacement plays a significant role in the stabilization. Other important effects include the mixing with unoccupied 4*s* and 4*p* orbitals of iron and 5*d* orbitals of the Ta^{5+} second-shell neighbors. As an important conclusion, the present analysis shows that the distortion in $KTaO_3:Fe^+$ is unrelated to steric effects often considered to be the origin of off-center movements in impurities. The detailed approach followed in this work for exploring a complex system can be useful for gaining a better insight into the origin of structural instabilities in pure and doped insulating materials.

DOI: 10.1103/PhysRevB.80.035131 PACS number(s): 71.55.−i, 61.72.Bb, 71.15.Mb, 71.70.Ch

I. INTRODUCTION

Since the discovery of the ferroelectricity in barium titanate in 1945,[1] a great deal of research has focused on understanding the nature and driving force of ferroelectric phase transitions in $BaTiO_3$ and other oxides. Many effects have been considered to be the origin of these structural instabilities, for instance, electrostatic interactions,[2–4] oxygen polarizability,[5,6] metal polarization,[4,7] the size of the ions,[8–11] lattice dynamics of a soft mode,[12] the coupling of vibrational and electronic (vibronic) freedom degrees,[13–16] and orbital hybridizations.[7,17–19] A great help for understanding the actual origin of the structural instability in pure oxides can be obtained from the study of spontaneous instabilities occurring in several transition-metal impurity centers in oxoperovskites.[20–25] Many of these studies have been focused on impurities in potassium tantalate, an incipient ferroelectric which remains cubic to zero temperature.[24–36] Research along this line requires fulfilling two main goals. In a first step it is necessary to determine experimentally and without any ambiguity the nature of the center and its associated instability. The cause responsible for the local distortion should be looked for in a second step.

Electron paramagnetic resonance (EPR) and electron-nuclear double resonance are, in principle, powerful techniques for clarifying the nature and structure of a paramagnetic center.[24–35] However, the superhyperfine interaction between unpaired electrons and ligand nuclei that provides with key information on the center can hardly be detected in oxides unless samples are highly enriched with ^{17}O whose natural abundance is 0.03%.[26–28] Furthermore, in the case of Kramers ions with a spin $S>1/2$ presenting a large zero-field splitting *only* the $|S,-1/2\rangle \rightarrow |S,1/2\rangle$ transition can be observed experimentally, so the associated EPR spectra are often described by an effective spin $S_{\text{eff}}=\frac{1}{2}$ smaller than the real S value for the electronic ground state.[26–28] A significant example in this realm concerns the axial iron center detected by EPR in $KTaO_3$.[26–35] This center is described by $S_{\text{eff}}=\frac{1}{2}$, $g_{\perp}^{\text{eff}}=4.33$, and $g_{\parallel}^{\text{eff}}=2.02$ and the principal direction associated with $g_{\parallel}^{\text{eff}}$ is a ⟨001⟩-type direction of the host lattice. Because of the experimental ratio between effective gyromagnetic constants ($g_{\parallel}^{\text{eff}}/g_{\perp}^{\text{eff}}\approx 4/2$), this center is sometimes referred to as the Fe4/2 center. As $g_{\perp}^{\text{eff}}=(S+1/2)g_{\perp}$,[26] it has been assumed that $S=3/2$. However, two very different models for the center have been put forward. While some authors[26,27] ascribed this center to a Fe^+ ($3d^7$) impurity at a K^+ site (called Fe_K^+ center, Fig. 1), experiencing an off-center motion along ⟨001⟩ directions, other groups[28,29] propose that the axial iron center involves a Fe^{5+} ($3d^3$) ion at a Ta^{5+} site (Fe_{Ta}^{5+}) which also undergoes an off-center shift along a principal direction of the $KTaO_3$ lattice.

We have recently shown[36] the usefulness of *ab initio* calculations to resolve these ambiguities. Indeed, density-functional-theory (DFT) calculations strongly support that the right model for the axial iron center is Fe_K^+ and not

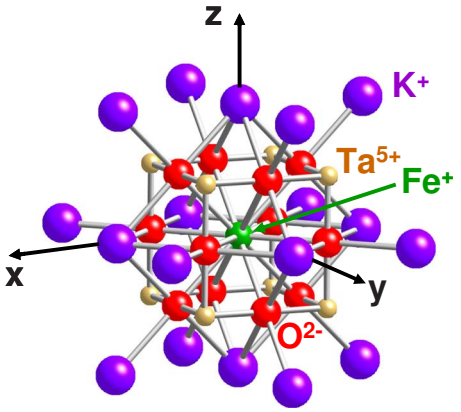

FIG. 1. (Color online) 39 atom cluster used in the calculations of the Fe_K^+ center in $KTaO_3$.

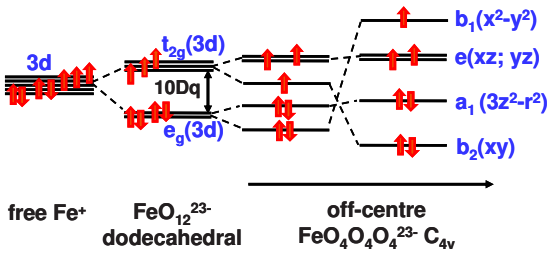

FIG. 2. (Color online) Qualitative scheme depicting the splitting of the mainly 3*d*(Fe) one-electron levels for dodecahedral FeO_{12}^{23-} (right) complexes and shift of the levels under a increasing Z_{Fe} off-center distortion of the Fe^+ cation, producing a $FeO_4O_4O_4^{23-}$ C_{4v} complex.

Fe_{Ta}^{5+}.[36] A central question is thus to understand why Fe^+ prefers not to remain at the K^+ site and make instead an off-center displacement close to 1 Å along a ⟨100⟩ direction of the $KTaO_3$ crystal. This work is just aimed at revealing the microscopic mechanisms responsible for such off-center instability. The obtained results shall be compared in a second step with the models which have already been described and that are commonly used to describe ferroelectric materials. Our starting point is the pseudo-Jahn–Teller (PJT) theory which, according to Bersuker,[37] is the only possible source of instability along an odd vibrational mode. In particular, we will use an orbital-based vibronic model[37] that we have previously tested on spontaneous instabilities with very different chemical nature, such as the symmetry change occurring in $BaF_2:Mn^{2+}$ at 55 K (Ref. 38) or the H-bond formation in $N_2H_7^+$ and $H_5O_2^+$ molecules.[39] This model allows us to determine the main molecular orbitals that are responsible for the distortion and to easily establish connections with other models such as polarization of the system's ions, hybridizations, etc.

Although a better insight into the mechanisms responsible for the off-center motion in the Fe_K^+ center in $KTaO_3$ can shed light on the origin of this kind of instabilities, this task is particularly difficult to achieve due to the following reasons: (1) at the on-center geometry, the Fe^+ ion presents an unusual dodecahedral coordination (FeO_{12} complex with octahedral symmetry, Fig. 1). Accordingly, in the off-center C_{4v} geometry there are three *distinct* groups of four oxygen ligands (called oxygen top, O_{top}, equatorial, O_{eq}, and bottom, O_{bot}, along this work) which couple in a different way to the Fe^+ orbitals. (2) The energy differences between antibonding levels are smaller than in cubic centers involving common 3*d* ions such as Cr^{3+}, Fe^{3+}, or Mn^{2+}. For example, the cubic-field splitting energy of Fe(3*d*) levels, $10Dq=\varepsilon(e_g)-\varepsilon(t_{2g})$, is equal only to −0.05 eV in this center (Fig. 2).[36] By contrast, $10Dq$ takes a value laying typically in the range of 1–3 eV for impurities such as Cr^{3+}, Fe^{3+}, or Ni^{2+} under octahedral coordination.[40] This situation thus favors the crossings of both orbital and electronic states' energies of the Fe_K^+ center in $KTaO_3$ when the geometry is varied. (3) At variance with what is found for free ions such as Cr^{3+} or Fe^{3+} the 4*s* and 4*p* orbitals are lying very close to 3*d* orbitals for the monovalent Fe^+ ion and thus they can also play a relevant role for explaining the equilibrium geometry and the associated electronic properties. More precisely, the 3*d*-4*p* separation for free Cr^{3+} or Fe^{3+} ions is around 20 eV while it is only about 2 eV for free Fe^+.[41] (4) Finally, due to the small band gap in $KTaO_3$, it is necessary to take into consideration unoccupied 5*d* orbitals of Ta to account for the stabilization of some orbitals of the Fe_K^+ center.

II. COMPUTATIONAL DETAILS

DFT calculations have been carried out by means of the Amsterdam density-functional (ADF) code[42] using various exchange-correlation functionals; the Vosko-Wild-Nusair[43] one in the local-density approximation (LDA) and the generalized gradient approximation (GGA) in its Becke-Perdew (BP) (Refs. 44 and 45) and Becke-Lee-Yang-Parr (BLYP) (Ref. 46) forms. The employed basis sets consists of three Slater-type orbitals plus a polarization function per atomic orbital as implemented in the ADF program. We used the basis that contained the larger frozen core available in the database as these orbitals play only a minor role in the studied properties.

Calculations for the Fe_K^+ center in $KTaO_3$ have been carried out using the cluster approximation. Previous results[47–50] obtained for Ni^+-, Cu^{2+}-, Ag^{2+}-, and Fe^+-doped MF_2 (M =Ca and Sr) and $SrCl_2$ showed that the off-center motion is well reproduced by small size clusters containing only 21 atoms because the active 3*d* electrons are localized to a good extent in the region formed by the impurity and ligands. In the present work, a $FeO_{12}Ta_8K_{18}^{47+}$ cluster of 39 ions centered at the Fe impurity (Fig. 1) has been used to simulate the Fe_K^+ center in $KTaO_3$. This cluster is thus the same previously used for deriving the equilibrium geometry and the electronic ground state of such a center.[36] In the geometry optimizations performed on all these clusters only the atomic positions of Fe ion and O ligands have been allowed to vary, the rest of ions being fixed at the experimental host-lattice positions. Calculations have been performed for clusters *in vacuo* as the electrostatic potential due to the rest of the lattice ions on the cluster region is found to be very flat in cubic oxoperovskites.[50]

In order to check the LDA and GGA results, some calculations were also carried out using the three parameter hybrid semiempirical B3LYP functional[51] implemented in the GAUSSIAN 98 package.[52] These calculations use the double zeta LANL2DZ basis, which contains Gaussian-type orbitals and pseudopotentials to simulate the core electrons. The obtained results are similar to the corresponding LDA and GGA values.

Atomic charges have been calculated along the ⟨001⟩ displacement of iron ion from the on-center position by means of three different charge analysis. Mulliken population analysis lead to unphysical results in the $FeO_{12}Ta_8K_{18}^{47+}$ cluster because of the large values of overlaps involving delocalized O^{2-} orbitals.[53] On the contrary, Voronoi and Hirshfeld charges, which prove to be numerically very similar,[53] yield physically meaningful charges.

III. RECALL OF VIBRONIC THEORY

Many authors have hypothesized that structural instabilities in pure and doped solids have a steric origin, i. e., due

only to atomic/ionic volumes. In the case of impurities in solids, the distortion would be associated to the substitution of an ion of the host network by a smaller impurity. However, experimental evidence contradicts this hypothesis. For example, EPR measurements indicate that a $3d^9$ cation as Cu^{2+} remains on-center in the CaF_2 lattice[54] while undergoes a small off-center $\langle 100\rangle$ displacement ($\sim$50 pm) in SrF_2,[54] and a huge displacement ($\sim$135 pm) in $SrCl_2$.[54] However, the isoelectronic Ni^+ cation gives rise to off-center $\langle 100\rangle$ displacements *in all* these lattices,[47] although this monovalent ion has a *larger size* than Cu^{2+}. In the case of the Fe_K^+ center in $KTaO_3$, the calculated value of the Fe-O distance keeping the Fe^+ ion at the on-center position is 278.3 pm only 5 pm smaller than the experimental K^+-O^{2-} distance (282 pm) in the host lattice.[36] Therefore, this small size difference is not able to explain the huge off-center displacement (93 pm) of the Fe^+ ion.

Supporting this view, previous *ab initio* studies on transition-metal impurities in solids have shown[36–38,47–50,54] that the occurrence of spontaneous off-center displacements in certain systems is the result of the subtle balance among several effects, some of them opposing and other favoring the movement of the impurity. Along this line it has been pointed out that the off-center motion of an impurity is favored by the flatness of the electrostatic potential, V_M, created by the rest of ions of the lattice simply taken as *point* charges.[36,38,47–50,54] For instance, in the case of the Fe_K^+ center in $KTaO_3$, the migration of the Fe^+ ion along a $\langle 100\rangle$-type direction until the equilibrium position $Z_{Fe}^0=93$ pm has been shown[36] to be helped by the flatness of $V_M(0,0,Z_{Fe})$, in the $0<Z_{Fe}<100$ pm domain.

According to the vibronic theory,[37] the instability of any nonlinear polyatomic system in a nondegenerate orbital state is driven by the *change in the electron density* with the distortion that allows overcoming the barrier associated with the breaking of bonds and electrostatic effects. The existence of instability can be checked through *ab initio* calculations obtaining the force constant, K, along the normal coordinate of the mode of interest, Q, at the high-symmetry configuration which is cubic in the case of the Fe_K^+ center in $KTaO_3$. If this force constant associated to the off-center displacement of Fe^+ is positive, the system will remain cubic while if the force constant is negative the Fe^+ ion will spontaneously displace off-center. To obtain K we expand the Hamiltonian $\hat{H}$ of the system with Q around the cubic configuration ($Q=0$)

$$\hat{H} \approx \hat{H}_0 + \frac{d\hat{H}}{dQ}Q + \frac{1}{2}\frac{d^2\hat{H}}{dQ^2}Q^2 + \cdots \tag{1}$$

Using now the *frozen* eigenfunctions, Ψ_i, of the Hamiltonian, H_0, at the cubic configuration the effect of the coordinate-dependent terms in Eq. (1) around $Q=0$ can be evaluated by means of perturbation theory. Then, the force constant of a given state, Ψ_0, can be written as[37]

$$K = K_0 + K_v \tag{2}$$

K_0 is called the primary force constant,

$$K_0 = \langle \Psi_0 | \frac{d^2\hat{H}}{dQ^2} | \Psi_0 \rangle \tag{3}$$

while K_v is the vibronic contribution to the force constant. Bersuker has proved[37] that, for cubic symmetry, K_0 is strictly positive and that it represents the force constant of the system when the electron density is *not allowed* to relax. On the other hand, K_v represents the vibronic coupling to the excited states at $Q=0$. The actual change in electron density is embodied in this admixture and, since K_0 is positive, it is the only possible source of distortion. We have developed a model where the key quantity, K_v, can, approximately, be written in terms of PJT couplings between orbitals[39,40]

$$K_v \approx \sum_{i\in occup} \sum_{j\in unoccup} (n_i - n_j) \frac{|\langle \phi_i | d\hat{H}/dQ | \phi_j \rangle|^2}{\Delta_{ij}}. \tag{4}$$

Here, n_i is the occupation of orbital i whose associated wave function is ϕ_i and Δ_{ij} is the energy necessary to excite one electron from orbital i to orbital j. It is important to note that, in the sum in Eq. (4), the index i runs over fully occupied orbitals while j index runs over semioccupied or unoccupied orbitals. As seen in Eq. (1) only couplings f_{ij},

$$f_{ij} = \langle \phi_i | dV/dQ | \phi_j \rangle \tag{5}$$

between orbitals with *different* occupations, $n_i \neq n_j$, contribute to the force constant. Accordingly it can be expected that for $KTaO_3$:Fe^+ the interaction between the mainly $3d$ levels which are *semioccupied* (Fig. 2) and the bonding counterparts play a role in the off-center displacement. Also the interaction between *empty* $4s$ (a_{1g}) and $4p$ (t_{1u}) orbitals and the antibonding $3d$ orbitals has been shown to play a relevant role in the instability of *monovalent* impurities.[49,50,54]

It is worthwhile to remark that, due to symmetry restrictions, not every orbital pair is allowed to interact since the vibronic constant f_{ij} is only non-null for certain combination of orbitals, i.e., the direct product of the irreducible representation (irrep) of ϕ_i and ϕ_j spans the irrep of Q. In particular for an off-center distortion the normal coordinate Q, and thus the dV/dQ operator in Eq. (5), is *odd* and the two orbitals ϕ_i and ϕ_j in Eq. (5) should have a *different* parity.

These non-null vibronic orbital couplings are directly related to the formation of bonding-antibonding orbital pairs that significantly change their energy along the distortion. This effect is usually referred as "hybridization" in the literature on ferroelectric instabilities[17,18] and our approach allows for a detailed analysis of its nature. Using symmetry-descend tables we are able to determine not only the symmetry of the orbitals that are allowed to couple but also the irrep to which each bonding-antibonding orbital pair arising from these couplings in C_{4v} symmetry belongs. Thus, for example, the $t_{2g}(3d)$ semioccupied orbital splits in e and b_2 components when the impurity moves off-center, so the bonding-antibonding partners of these orbitals have to belong to a_{2u}, e_u, t_{1u}, or t_{2u} in cubic symmetry since these are the only irreps coupled to t_{2g} through a t_{1u} vibration.

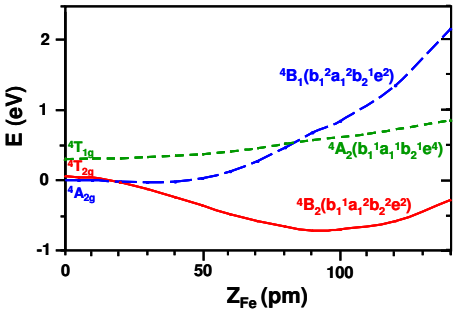

FIG. 3. (Color online) Profiles of the DFT total energy of the C_{4v} Fe_K^+ center in $KTaO_3$ as a function of the Z_{Fe} coordinate calculated for $^4B_1[b_1(x^2\text{-}y^2)^2a_1(3z^2\text{-}r^2)^2b_2(xy)^1e(xz,yz)^2]$, $^4B_2[b_1(x^2\text{-}y^2)^1a_1(3z^2\text{-}r^2)^2b_2(xy)^2e(xz,yz)^2]$, and $^4A_2[b_1(x^2\text{-}y^2)^1a_1(3z^2\text{-}r^2)^1b_2(xy)^1e(xz,yz)^4]$ states of the complex coming, respectively, from the ground state $^4A_{2g}$ and the excited states $^4T_{2g}$ and $^4T_{1g}$ in the on-center (O_h) geometry.

IV. RESULTS AND DISCUSSION

Seeking to clarify the microscopic origin of the off-center distortion in the Fe_K^+ center in $KTaO_3$ let us explore the evolution of relevant valence orbitals and some electronic states with the distortion coordinate, Z_{Fe}. Main results are displayed in Figs. 4–7.

As it was previously noted[36] the off-center distortion is strongly dependent on the electronic state (Fig. 3). In fact, the electronic configuration of Fe^+ at the stable equilibrium geometry in $KTaO_3$ is different from $^4A_{2g}(e_g^4t_{2g}^3)$ corresponding to the ground state of Fe^+ in a perfect cubic symmetry. When the Fe^+ ion is displaced from the K^+ site the electronic $^4A_{2g}(e_g^4t_{2g}^3)$ state presents only a very *shallow* off-center minimum at around $Z_{Fe} \approx 0.37$ Å (Fig. 3). However, the first

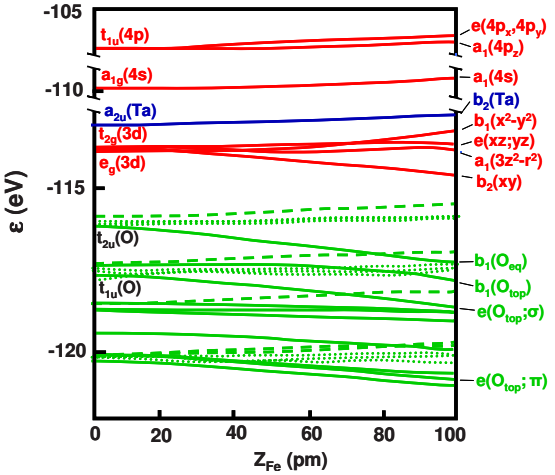

FIG. 4. (Color online) Energy profiles obtained from DFT-BP calculations for the relevant molecular orbitals of the $FeO_{12}Ta_8K_{18}^{47+}$ cluster along the $O_h \rightarrow C_{4v}$ off-center instability. Labels at the left (right) part of the picture correspond to O_h (C_{4v}) complex. Solid red lines correspond to orbitals with mainly Fe character (3*d*, 4*s*, and 4*p*) while a relevant orbital with Ta character is depicted in solid blue line. Orbital energies of mainly O_{top}, O_{bot}, and O_{eq} orbitals are depicted with green solid, green dashed, and green dotted lines, respectively.

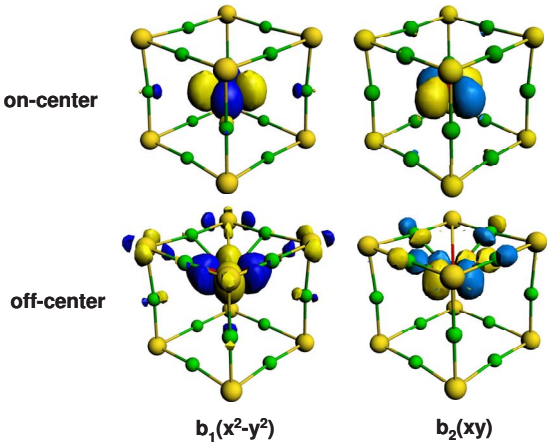

FIG. 5. (Color online) Pictures of $b_1(x^2\text{-}y^2)$ (left) and $b_2(xy)$ orbitals (right), with mainly 3*d*(Fe) character, in on-center (up) and off-center (down) geometries.

excited state in O_h symmetry, $^4T_{2g}$, lying at only 0.06 eV above $^4A_{2g}$, splits into $^4E(b_1^1a_1^2e^3b_2^1)$ and $^4B_2(b_1^1a_1^2e^2b_2^2)$ components when the symmetry descends to C_{4v}. Here b_1, a_1, e, and b_2 are orbitals with mainly $3d_{x2-y2}$, $3d_{3z2-r2}$, $3d_{xz}$-$3d_{yz}$, and $3d_{xy}$ character, respectively. The $^4B_2$ state can be obtained from the electronic configuration of $^4A_{2g}$ by excitation of one electron from the $b_1(x^2\text{-}y^2)$ orbital to the $b_2(xy)$ one and exhibits a very large off-center stabilization energy of ~0.7 eV so that it becomes the actual ground state when $Z_{Fe} > 0.15$ Å (Fig. 3).

The crossing of $^4B_1(b_1^2a_1^2e^2b_2^1)$ and $^4B_2(b_1^1a_1^2e^2b_2^2)$ states is directly related to the quite different evolution followed by the energies of $b_1(x^2\text{-}y^2)$ and $b_2(xy)$ orbitals (Fig. 4) with the distortion coordinate, Z_{Fe}. We can see in Fig. 4 that the energy of $b_1(x^2\text{-}y^2)$ orbital increases with the distortion while $b_2(xy)$ descends with it. This effect can be understood observing that in the on-center geometry the $3d_{xy}$(Fe) orbital is directed toward the equatorial ligands (Fig. 5) and thus has a pure σ-bonding character. On the other hand, in that situa-

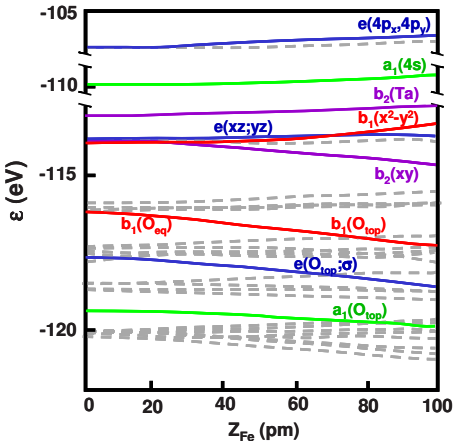

FIG. 6. (Color online) Modification of Fig. 4 in order to highlight in solid lines the most relevant orbital couplings giving rise to bonding-antibonding orbital pairs. Coupling of e, a_1, b_2, and b_1 orbitals are represent by means of blue, green, pink, and red lines, respectively.

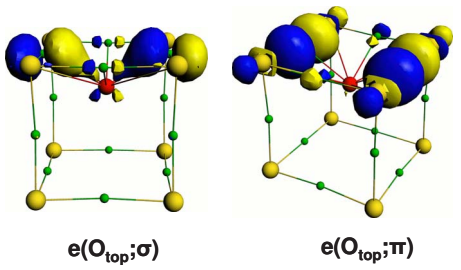

FIG. 7. (Color online) Pictures of $e(O_{top};\sigma)$ and $e(O_{top};\pi)$ orbitals represented at the off-center geometry. The admixture between $2p$ oxygen orbitals and $5d$(Ta) orbitals in $e(O_{top};\pi)$ is clearly seen.

tion, the $3d_{x2-y2}$(Fe) orbital points toward the interstices between the ligands and does not have σ-bonding character with the equatorial ligands (Fig. 5). However, when the Fe^+ ion is displaced the $b_2(xy)$ orbital partially loses its σ character and $b_1(x^2\text{-}y^2)$ gains it since the squares formed by equatorial and top ligands are rotated 45° with respect to each other (Fig. 5). In the spirit of Eq. (4), one should expect that a strong increase or descend in energy of an orbital can only occur if there is mixing, respectively, with a bonding or antibonding partner. This is just what is seen in Figs. 4 and 6, where the increase in energy in $b_1(x^2\text{-}y^2)$ is clearly accompanied by a strong descend in energy of $b_1(O_{top})$ orbital [coming from t_{2u}(O) ligand levels in O_h symmetry] and thus both levels form a bonding-antibonding pair. This $e_g(3d)$-t_{2u}(O) coupling, forbidden in O_h symmetry becomes allowed under the C_{4v} distortion. Another direct proof of such a PJT coupling is thus obtained looking at the $3d_{x2-y2}$(Fe) admixture into the bonding $b_1(O_{top})$ orbital which amounts to 8.4% at Z^0_{Fe}=93 pm.

Let us now focus on the $b_2(xy)$ orbital which also plays an important role. As a salient feature the decrease in energy of $b_2(xy)$ can be correlated with the increase in energy of an empty b_2(Ta) orbital rather (Figs. 4 and 6) than with the energy variation in the $b_2(O_{eq})$ orbital mainly made of equatorial ligands. Indeed, checking the contribution of Ta to the wave function of $b_2(xy)$ we observe an increase from 9% to nearly 20% when iron is displaced from Z_{Fe}=0 to Z^0_{Fe} =93 pm. It is worth noting that the $b_2(xy)$ orbital has a *bonding* character with respect to the admixture between $3d_{xy}$(Fe) and b_2(Ta) orbitals while it exhibits an antibonding character when considering hybridization between $3d_{xy}$(Fe) and oxygen-ligand orbitals. This mixing is clearly observable in Fig. 5, where the $b_2(xy)$ orbital shows a bonding interaction of the $3d_{xy}$(Fe) orbital with the d orbitals of the Ta ions placed on the top vertex of the $O_{12}Ta_8$ cube.

It is important to note that both orbital mixings, $b_1(x^2\text{-}y^2)$-$b_1(O_{top})$ and b_2(Ta)-$b_2(xy)$, are allowed by symmetry according to Eq. (6). In the first case, the fully occupied orbital comes from the splitting of a t_{2u}(O) orbital which is allowed to couple to the $e_g(3d)$ one from where $b_1(x^2\text{-}y^2)$ comes (Fig. 4), while in the second the $t_{2g}(3d)$ can couple to the a_{2u}(Ta) orbital.

Looking now at the evolution with Z of the different orbitals (Fig. 6) and the mechanism of energy reduction through vibronic coupling it is already possible to understand why the well in the $^4B_2(b_1^1a_1^2e^2b_2^2)$ state is much deeper than for $^4B_1(b_1^2a_1^2e^2b_2^1)$ corresponding to the ground state when Z=0 as shown in Fig. 3. In Sec. III it was pointed out that when two orbitals are coupled by the vibronic operator dV/dQ there is an energy gain in the ground state if such orbitals are *not equally populated*. For this reason the important $b_1(x^2\text{-}y^2)$-$b_1(O_{top})$ interaction has no effect in the $^4B_1(b_1^2a_1^2e^2b_2^1)$ state where the antibonding $b_1(x^2\text{-}y^2)$ is fully occupied. For a similar reason the b_2(Ta)-$b_2(xy)$ interaction is more important for the $^4B_2(b_1^1a_1^2e^2b_2^2)$ than for the $^4B_1(b_1^2a_1^2e^2b_2^1)$ state.

We have also found an important PJT contribution coming from the mixing of the $4s$(Fe) orbital with an oxygen t_{1u} one. This can be seen in the strong mixing of the unoccupied $a_{1g}(4s)$ orbital of 5.2% into the t_{1u}(O) orbital.

Observing Fig. 4 we can see that the orbital energies of the ligands behave differently when Z_{Fe} increases depending on whether they are composed of top, equatorial, or bottom groups of oxygen ligands. The energy of O_{bot} orbitals increases when the distortion is realized, for O_{eq} it is almost constant, while for O_{top} it reduces. This fact shows that O_{bot} ligands are losing bonding while O_{top} ones become bonding. Apart from the energy decrease in $b_1(O_{top})$ and $a_1(O_{top})$ mainly ligand orbitals a similar situation is encountered (Fig. 4) when looking at $e(O_{top};\sigma)$ and $e(O_{top};\pi)$ orbitals depicted in Fig. 7. We have verified that the main mechanism for decreasing the energy of the $e(O_{top};\sigma)$ orbital comes from the interaction with the antibonding $e(xz,yz)$ orbital (Figs. 4 and 7). Indeed there is an admixture of 5.72% of $3d_{xz}$(Fe) $-3d_{yz}$(Fe) character into the $e(O_{top};\sigma)$ orbital at the equilibrium geometry while that arising from $4p$(Fe) orbitals amounts only to 0.44%.

A different situation is encountered when looking at the $e(O_{top};\pi)$ orbital depicted in Figs. 4 and 7. That orbital when Z_{Fe}=0 is mainly made of top oxygen (75%) and $4d$(Ta) (20%). When the distortion takes place there is a progressive contamination of $4p$(Fe) in the wave function which becomes close to 2% for Z^0_{Fe}=93 pm. According to this analysis the antibonding $e(xz,yz)$ orbital in Fig. 6 is pressed upward by the bonding $e(O_{top};\sigma)$ while downward by the unoccupied $e(4p)$ mainly made of $4p$(Fe). Indeed we have verified that there is a ~1% admixture of $4p$(Fe) into the antibonding $e(xz,yz)$ orbital. This explains, albeit qualitatively, the small dependence of its associated energy on Z_{Fe} (Fig. 6). Bearing in mind that the $e(O_{top};\sigma)$ orbital is fully occupied while the antibonding $e(xz,yz)$ orbital is half filled this also helps to stabilize the off-center distortion.

The present analysis supports that the off-center instability for Fe^+ in $KTaO_3$ is sustained by significant changes in the chemical bonding. This relevant fact is also well seen when looking at the variation in charge on different ions as a function of Z_{Fe}. Our calculations reveal that O_{bot} ligands gain charge as the result of a decreased covalency with the Fe^+ ion, O_{eq} maintain their charge while O_{top} lose charge due an increased covalency with iron. However, the largest change in charge takes place on the metal that receives almost 0.15 electrons due to an increased covalency with O_{top} oxygens (Fig. 8). We can further divide the charge transfer onto the metal in s, p, and d components, as shown in Fig. 8. It is found that the main transfer channel is the $4s$ orbital consis-

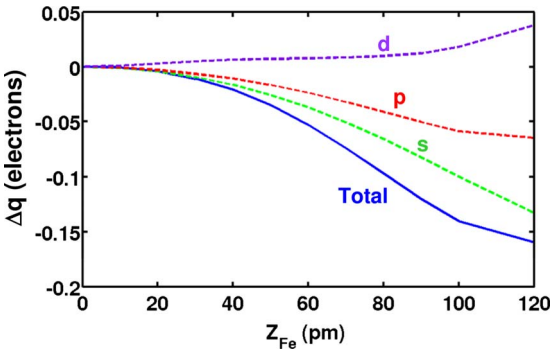

FIG. 8. (Color online) Variation in the atomic charge on Fe along the Z_{Fe} coordinate and partial *s*, *p*, and *d* contributions.

tent with a large $a_{1g}(4s)$-$t_{1u}(O)$ coupling, as indicated above.

It is worth noting now that there are significant differences between the apparently similar $SrCl_2:Fe^+$ center[49] and the present system where the situation is certainly more complex. For instance, in $SrCl_2:Fe^+$ there are no equatorial ligands while top and bottom ligands are placed in the apex of the cube formed by such anions.[49] This fact implies that there is no σ bonding in the $b_1(x^2\text{-}y^2)$ orbital corresponding to $SrCl_2:Fe^+$. Also, $SrCl_2$ is a large-gap insulator where the band-gap energy is ~7.5 eV (Ref. 55) and levels from Sr do not play a relevant role for understanding the distortion. However, in $KTaO_3$ the band gap is only 3.6 eV (Ref. 56) and 5*d*(Ta) orbitals can actively participate in the distortion of the system. Along this line the lack of chemical bonding for the mainly $e(xz,yz)$ orbitals in $SrCl_2:Fe^+$ gives rise to a significant decrease in its energy when Z_{Fe} increases due to the vibronic interaction with 4*p*(Fe).

V. FINAL REMARKS

This paper has conducted an analysis of the microscopic origin of the off-center instability suffered by Fe^+ impurities replacing K^+ ions in $KTaO_3$. Results of this study demonstrate, first, that off-center instabilities are directly related to changes in bonding associated with the displacement of ions. Therefore, this work rules out the possibility of a steric origin due to substitution of an ion from the host lattice by a smaller impurity. Moreover, the present results show that a study of the evolution of orbitals with the distortion coordinate where symmetry considerations are taken into account is a useful tool for gaining a better insight into the origin of any structural instability. This *detailed* approach can thus be applied to explore the origin of structural instabilities around impurities and also in pure insulating materials (for example, in the case of ferroelectric phase transitions).

The analysis carried out on $KTaO_3:Fe^+$ points out the complexity of the problem involving not a single pair but several levels whose energy increases or decreases due to vibronic interactions. Leaving aside the relevant role played by 4*s* and 4*p* orbitals of Fe^+ it is worthwhile to remark the importance of the empty 5*d* levels of Ta in bonding and structural properties. This result is unusual since the covalent-bond formation with second-shell neighbors has never, to our knowledge, been pointed out to play any role in the off-center displacement of an impurity. It should be noted that superhyperfine interaction with Ta nuclei has been found in EPR experiments,[28] a fact which supports albeit qualitatively that Ta levels are involved in bonding. Further study on this matter is however necessary.

In the study of instabilities simple concepts such as polarization on a given atom concepts are widely used. The present results underline that such simple concepts are not adequately defined. On the other hand the general pseudo-Jahn–Teller approach offers the flexibility to describe and analyze all changes in electron density when a distortion is underway. The latter reasoning implies that studies of the changes in the electron density when the system moves from $Q=0$ to a distorted situation should cast some light on the force responsible for the distortion. Work along this relevant issue is now underway.

ACKNOWLEDGMENT

The support by the Spanish Ministerio de Ciencia y Tecnología under Project No. FIS2006-02261 is acknowledged.

[1] A. Von Hippel, R. G. Breckenridge, F. G. Chesley, and L. Tisza, Ind. Eng. Chem. **38**, 1097 (1946).
[2] W. P. Mason and B. T. Matthias, Phys. Rev. **74**, 1622 (1948).
[3] J. C. Slater, Phys. Rev. **78**, 748 (1950).
[4] B. B. van Aken, T. M. Palstra, A. Filipetti, and N. A. Spaldin, Nature Mater. **3**, 164 (2004).
[5] R. Migoni, H. Bilz, and D. Baüerle, Phys. Rev. Lett. **37**, 1155 (1976).
[6] A. Bussmann-Holder and H. Büttner, Nature (London) **360**, 541 (1992).
[7] D. I. Khomskii, J. Magn. Magn. Mater. **306**, 1 (2006).
[8] N. W. Thomas, Acta Crystallogr., Sect. B: Struct. Sci. **45**, 337 (1989).
[9] M. Kunz and I. D. Brown, J. Solid State Chem. **115**, 395 (1995).
[10] R. C. Buchanan and T. Park, *Materials Crystal Chemistry* (CRC, Cleveland/Boca Raton, 1997).
[11] U. Adem, A. A. Nugroho, A. Meetsma, and T. T. M. Palstra, Phys. Rev. B **75**, 014108 (2007).
[12] W. Cochran, Adv. Phys. **9**, 387 (1960).
[13] I. B. Bersuker, Phys. Lett. **20**, 589 (1966).
[14] R. A. Wheeler, M.-H. Whangbo, T. Hughbanks, R. Hoffmann, J. K. Burdett, and T. A. Albright, J. Am. Chem. Soc. **108**, 2222 (1986).
[15] R. Seshadri and N. A. Hill, Chem. Mater. **13**, 2892 (2001).
[16] P. Baettig, C. F. Schelle, R. LeSar, U. V. Waghmare, and N. A. Spaldin, Chem. Mater. **17**, 1376 (2005).
[17] R. E. Cohen and H. Krakauer, Phys. Rev. B **42**, 6416 (1990).
[18] R. E. Cohen, Nature (London) **358**, 136 (1992).

[19] D.-Y. Cho, J.-Y. Kim, B.-G. Park, K.-J. Rho, J.-H. Park, H.-J. Noh, B. J. Kim, S.-J. Oh, H.-M. Park, J.-S. Ahn, H. Ishibashi, S.-W. Cheong, J. H. Lee, P. Murugavel, T. W. Noh, A. Tanaka, and T. Jo, Phys. Rev. Lett. **98**, 217601 (2007).
[20] E. Siegel and K. A. Muller, Phys. Rev. B **20**, 3587 (1979).
[21] K. A. Müller and W. Berlinger, Phys. Rev. B **34**, 6130 (1986).
[22] A. Tkach, P. M. Vilarinho, and A. Kholkin, Appl. Phys. Lett. **86**, 172902 (2005).
[23] G. Volkel and K. A. Muller, Phys. Rev. B **76**, 094105 (2007).
[24] B. E. Vugmeister and M. D. Glinchuk, Sov. Phys. Usp. **28**, 589 (1985).
[25] B. E. Vugmeister and M. D. Glinchuk, Rev. Mod. Phys. **62**, 993 (1990).
[26] M. D. Glinchuk, V. V. Laguta, I. P. Bykov, J. Rosa, and L. Jastrabík, Chem. Phys. Lett. **232**, 232 (1995).
[27] M. D. Glinchuk, V. V. Laguta, I. P. Bykov, J. Rosa, and L. Jastrabík, J. Phys.: Condens. Matter **7**, 2605 (1995).
[28] P. G. Baranov, A. G. Badalyan, D. V. Azamat, V. A. Trepakov, A. P. Bundakova, E. A. Ruzanova, and V. S. Vikhnin, Phys. Rev. B **74**, 054111 (2006).
[29] V. E. Bursian, V. S. Vikhnin, L. S. Sochava, S. Kapphan, and H. Hesse, Phys. Solid State **39**, 547 (1997).
[30] M. M. Abraham, L. A. Boatner, D. N. Olson, and U. T. Höchli, J. Chem. Phys. **81**, 2528 (1984).
[31] V. V. Laguta, M. D. Glinchuk, I. P. Bykov, J. Rosa, L. Jastrabík, R. S. Klein, and G. E. Kugel, Phys. Rev. B **52**, 7102 (1995).
[32] H.-J. Reyher, B. Faust, M. Maiwald, and H. Hesse, Appl. Phys. B: Lasers Opt. **63**, 331 (1996).
[33] V. V. Laguta, M. D. Glinchuk, I. P. Bykov, J. Rosa, L. Jastrabík, M. Savinov, and Z. Trybula, Phys. Rev. B **61**, 3897 (2000).
[34] K. Leung, Phys. Rev. B **65**, 012102 (2001).
[35] E. L. Venturini, G. A. Samara, V. V. Laguta, M. D. Glinchuk, and I. V. Kondakova, Phys. Rev. B **71**, 094111 (2005).
[36] A. Trueba, P. García-Fernández, J. M. García-Lastra, M. T. Barriuso, J. A. Aramburu, and M. Moreno, Phys. Rev. B **78**, 085122 (2008).
[37] I. B. Bersuker, *The Jahn-Teller Effect* (Cambridge University Press, Cambridge, 2006).
[38] P. García-Fernández, J. A. Aramburu, M. T. Barriuso, and M. Moreno, J. Chem. Phys. **128**, 124513 (2008).
[39] P. García-Fernández, L. García-Canales, J. M. García-Lastra, J. Junquera, M. Moreno, and J. A. Aramburu, J. Chem. Phys. **129**, 124313 (2008).
[40] A. Abragam and B. Bleaney, *Electron Paramagnetic Resonance of Transition Ions* (Clarendon, Oxford, 1970).
[41] C. E. Moore, Natl. Stand. Ref. Data Ser. (U.S., Natl. Bur. Stand.) **35**, 1 (1971).
[42] G. T. Velde, F. M. Bickelhaupt, E. J. Baerends, C. F. Guerra, S. J. A. Van Gisbergen, J. G. Snijders, and T. Ziegler, J. Comput. Chem. **22**, 931 (2001).
[43] S. H. Vosko, L. Wilk, and M. Nusair, Can. J. Phys. **58**, 1200 (1980).
[44] A. D. Becke, Phys. Rev. A **38**, 3098 (1988).
[45] J. P. Perdew, Phys. Rev. B **33**, 8822 (1986).
[46] C. Lee, W. Yang, and R. G. Parr, Phys. Rev. B **37**, 785 (1988).
[47] P. García-Fernández, J. A. Aramburu, M. T. Barriuso, and M. Moreno, Phys. Rev. B **69**, 174110 (2004).
[48] P. García-Fernández, J. A. Aramburu, M. Moreno, and M. T. Barriuso, J. Chem. Phys. **129**, 187101 (2008).
[49] P. García-Fernández, J. A. Aramburu, M. T. Barriuso, and M. Moreno, Phys. Rev. B **73**, 184122 (2006).
[50] M. Moreno, M. T. Barriuso, J. A. Aramburu, J. M. García-Fernandez, and J. M. García-Lastra, J. Phys.: Condens. Matter **18**, R315 (2006).
[51] A. D. Becke, J. Chem. Phys. **98**, 5648 (1993).
[52] GAUSSIAN 98, M. J. Frisch *et al.*, Gaussian Inc., Pittsburgh PA, 1998.
[53] C. Fonseca Guerra, J.-W. Handgraaf, E. J. Baerends, and F. M. Bickelhaupt, J. Comput. Chem. **25**, 189 (2004).
[54] J. A. Aramburu, P. García Fernández, M. T. Barriuso, and M. Moreno, Phys. Rev. B **67**, 020101 (2003).
[55] C. Sugiura, Phys. Rev. B **9**, 2679 (1974).
[56] G. E. Jellison, I. Paulauskas, L. Boatner, and D. J. Singh, Phys. Rev. B **74**, 155130 (2006).